Journal of Applied Polymer Science

Preparation, dynamic rheological behavior, crystallization, and mechanical properties of inorganic whiskers reinforced polylactic acid/hydroxyapatite nanocomposites

Zhuo Liu, Yinghong Chen, Weiwei Ding
State Key Laboratory of Polymer Materials Engineering (Sichuan University), Polymer Research Institute of Sichuan University, Chengdu 610065, China
Correspondence to: Y. Chen (E-mail: johnchen@scu.edu.cn)

ABSTRACT: The novel inorganic SiO_2–MgO–CaO whiskers (SMCWs) were incorporated into nano hydroxyapatite (HA) contained polylactic acid (PLA) system to prepare the reinforced PLA/HA/SMCWs nanocomposite. Maleic anhydride grafted PLA (PLA-*g*-MAH) was then used to modify the interface between filler and matrix. The morphology, rheological behavior, crystallization, and mechanical property of the prepared nanocomposites were systematically investigated using scanning electronic microscope, dynamic rheometer, differential scanning calorimeter, polarized light microscope, and mechanical test, respectively. The results showed that the introduced PLA-*g*-MAH obviously improves the filler dispersion and the filler–matrix interfacial compatibility. Interestingly, the incorporated whiskers obviously decrease the complex viscosity and hence could significantly improve the processability of system. However, the introduction of PLA-*g*-MAH increases the complex viscosity to a greater extent. In addition, the added whiskers were found to have complicated influences on the PLA crystallization. On one hand, the incorporated whiskers can enhance the melt crystallization capability of PLA macromolecular chains; on the other hand, the introduced whiskers also show the inhibitive effect on the nucleation of PLA polymer chains and the inhibition degree is related to the loading of whiskers. The combination of whiskers and PLA-*g*-MAH could remarkably improve the mechanical performance of PLA/HA nanocomposite. © 2016 Wiley Periodicals, Inc. J. Appl. Polym. Sci. **2016**, *133*, 43381.

KEYWORDS: biodegradable; composites; crystallization; mechanical properties; rheology

Received 22 October 2015; accepted 22 December 2015
DOI: 10.1002/app.43381

INTRODUCTION

Polylactic acid (PLA) is completely biodegradable and synthesized from the direct condensation polymerization of naturally produced lactic acid or by catalytic ring-opening polymerization of the corresponding lactide. PLA has many advantages, such as good biocompatibility, good mechanical performance, easy processing, no toxicity, bioresorbability, etc. and therefore has been regarded as the most promising biodegradable polymer materials with environmentally benign features. PLA has broad applications, e.g., in preparation of biodegradable fibers and plastic parts, drug sustained-release material, surgical suture, scaffolds, and ophthalmic materials, etc.[1–10] In the biomedical area, PLA indeed shows some important application prospects. However, when used in preparation of materials for bone tissue repair, PLA still exhibits some disadvantages,[11–13] such as poor toughness, unfavorable acidic degradation product formed in human body, no osteoconduction, etc. This of course obviously does not benefit the bone tissue repair.

Currently, there have been various methods applied to modify PLA.[14–16] The incorporation of hydroxyapatite (HA) nanoparticles is one of the effective ways. As is well known, HA, as the main inorganic component of the human bone, is an important inorganic material with excellent bioactivity, biocompatibility, and osteoconductivity. It could, therefore, induce the bone growth. However, HA has poor processability and is hard to be shaped. Obviously, compositing of PLA with HA could sufficiently combine their respective advantages. This combination can help to tune the initial mechanical strength and the decay rate and also delay the early degradation of PLA. In addition, the weak alkali component of HA can neutralize the acidic products produced during PLA degradation occurring in the human body. PLA/HA composite proves to have a structure similar to natural bone and thus shows a potential to induce the osteogenesis and a good biocompatibility. As a consequence, in biomedical area (particularly bone tissue repair field), much attention has been paid to preparation of PLA/HA biocomposite. In recent years, there are more and more related

investigations conducted.[17–30] For example, Jiang *et al.*[20] investigated the influence of HA with different grain size on the crystallization behavior and mechanical property of HA/PLA composite. They found that compared with HA with small grain size range, the HA with lager grain size range is more beneficial to promotion of crystallization of PLA and can hence result in a higher mechanical property of HA/PLA composite. Dadbin *et al.*[25] prepared PLA/HA nanocomposite films using solution casting method and the films were then irradiated with γ rays. The results showed that compared with unirradiated PLA/HA nanocomposite, the irradiated nancomposite has α PLA crystalline phase and higher tensile strength. Liu *et al.*[28] utilized a melt-compounding process to fabricate HA nanorods and silver nanoparticles incorporated in biodegradable PLA composite. The prepared composite hybrids with low Ag content show good biocompatibility and maintain a good balance between antibacterial activity and cytocompatibility. However, there are still challenges in the prepared PLA/HA composites, e.g., their mechanical properties cannot satisfy the requirements of the massive bones for the fixation strength. In order to obtain the enhanced mechanical performance, the PLA/HA composite still needs modification so that it can be better applied in bone repair field.

The inorganic whisker, a high-strength fiber grown from a single crystal under certain conditions, is a kind of ideal fiber-like filler for polymer reinforcement due to its extremely high strength. SiO_2–MgO–CaO whisker (SMCW), with a chemical structural formula of $Ca_2Mg_5[Si_8O_{22}](OH)_2{\cdot}n\{CaMg[Si_2O_6]{\cdot}0.3Mg_2[Si_2O_6]\}$ (n = 0.05–0.1), is a novel high-performance inorganic silicate reinforcing filler with a radial size in micrometer and low cost. It has an aspect ratio of 20–80 and hence a very high mechanical property (the corresponding tensile strength and tensile modulus could even reach 1.2 and 32 GPa, respectively).[31] There have been several studies on preparation of SMCW reinforced polymer composite, e.g., high-density polyethylene (HDPE)/SMCW composite,[32] polypropylene (PP)/SMCW composite,[33] etc. So, the SMCW could be a good candidate to be used to reinforce PLA/HA composite. As a kind of whisker, SMCW may cause the potential health hazard due to its shape and size, e.g., silicose disease, etc.[34,35] However, such a risk could be avoided by melt compounding of SMCWs with polymer and introduction of maleic anhydride grafted polymer (enhancing the combination of whisker with polymer matrix).

To the best of our knowledge, there is no similar work done on SMCW reinforced PLA/HA composite system. Introduction of a small amount of SMCWs into PLA/HA composite system not only can further improve the mechanical properties but also can have the virtues of PLA/HA biocomposites. In the present work, an attempt to use SMCW as a reinforced phase to prepare PLA/HA/SMCW composite was made for the first time. Considering the relatively poor filler–matrix interactions, maleic anhydride grafted PLA (PLA-*g*-MAH) was introduced to enhance the interfacial bonding. This paper mainly focuses on the investigation of the rheological behavior, crystallization behavior and mechanical properties of PLA/HA/SMCW composite. The other important properties of the composite such as biocompatibility, biodegradability, etc., will be investigated later.

EXPERIMENTAL

Materials

PLA (4032D) with a glass transition temperature of 50–55 °C and a melting temperature of 165–170 °C was supplied by Suzhou Youli Technology Material Corporation. It has a melt flow index of 3.87 g (10 min)$^{-1}$ (190 °C, 2.16 kg). Hydroxyapatite (HA) with diameter in the range of 20–40 nm was purchased from Nanjing Emperor Nano Material Corporation. SMCW with diameter in the range of 0.2–2 μm and length in the range of 5–50 μm, made from the tremolite, was provided by Mianyang Guangda Company. Maleic anhydride grafted polylactic acid (PLA-*g*-MAH) with 1.2% grafting rate was prepared by ourselves.

Sample Preparation

The maleic anhydride grafted polylactic acid was prepared through reactive extrusion. Firstly, a 0.05 g/mL acetone solution containing maleic anhydride (MAH) and dicumyl peroxide (DCP) (MAH:DCP = 4:1, weight ratio) was prepared by dissolving MAH and DCP in acetone. Then, the prepared acetone solution was added to the dried PLA pellets in a weight ratio of PLA:(MAH + DCP) = 98:2.5 with a good mixing and let the acetone completely evaporated. The obtained PLA pellets coated with MAH and DCP were reactively extruded in a TSSJ-25/33 co-rotating twin-screw extruder (ϕ = 25 mm, L/D = 33, Chenguang Research Institute of Chemical Industry). The extrudates were cooled, pelletized, and dried and the PLA-*g*-MAH pellets were finally obtained. FT-IR characterization was conducted on the prepared PLA-*g*-MAH. Before measurement, the prepared PLA-*g*-MAH was extracted in a Soxhlet extractor using acetone for 24 h to remove the unreacted MAH. FT-IR analyses (the measurement results can be found in the mechanical property part) show that compared with pure PLA, the prepared PLA-*g*-MAH has significantly weakened stretching vibration absorptions of C—H group in PLA at 2998 cm^{-1} and obviously enhanced stretching vibration absorptions of —CH_2— group in grafted MAH at 2924 and 2851 cm^{-1}. The stretching absorption of C═O group in grafted MAH at 1760 cm^{-1} was overlapped by that of C═O group in PLA. Above results indicate the successful preparation of PLA-*g*-MAH. The grafting rate proves to be 1.2% using titration method. The grafting reaction of MAH on to PLA chains was shown in Figure 1.

For preparation of the PLA composites, the dried ingredients with formulation composition shown in Table I were mixed in a high-speed mixer. Then, the well-mixed ingredients were extruded at 170–180 °C in a TSSJ-25/33 corotating twin-screw extruder (ϕ = 25 mm, L/D = 33, Chenguang Research Institute of Chemical Industry). The cooled extrudates were cut into pellets and then dried in an oven at 80 °C for 6 h. The dried pellets were molded into standard samples for tests using an injection molding machine (K-TEC 40, Terromatik Milacron Corporation) at melt temperature of 190 °C. The sample names corresponding to various formulations are also given in Table I.

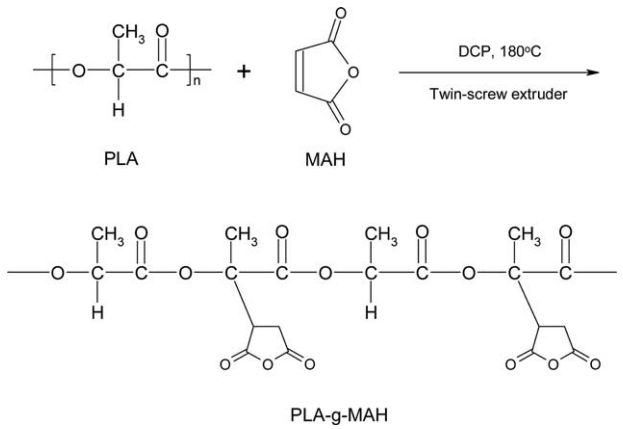

Figure 1. The proposed grafting reaction of PLA with MAH in twin-screw extruder.

Characterization

The morphology of fractured surface of different sample was observed on an INSPECT F scanning electron microscope (SEM) (FEI Company, Japan) with an acceleration voltage of 20 kV. Before observation, the cryogenically fractured surface of sample was coated with a thin gold layer. The rheological measurements were performed on a Bohin Gemini 200 dynamic rheometer (Marvin Corporation) using a set of parallel plates with 2.5 cm diameter and 1.0 mm gap. The used samples with 1 mm thickness and 2 mm diameter were firstly heated to 190 °C and kept for 5 min to eliminate the original crystalline structures and then cooled quickly to 180 °C. The dynamic frequency sweep was carried out under conditions of frequency range, strain amplitude, and temperature being 0.025–100 rad s^{-1}, 1 and 180 °C, respectively. A TA Q20 differential scanning calorimeter (DSC) (TA Company) was used to analyze the melting and crystallization behavior of different samples. The samples (about 8 mg) were heated from 40 to 200 °C with a heating rate of 10 °C min^{-1} and then cooled to 40 °C with a cooling rate of 20 °C min^{-1} under nitrogen atmosphere. A DM 2500p polarizing light microscope (PLM) (Leica Corporation) equipped with a hot-stage was used to observe the isothermal crystallization morphologies of different samples. The test sample placed between both glass slices was heated to 200 °C at a heating rate 30 °C min^{-1} and let the sample adequately melted. The molten sample could form a very thin film between the both glasses. Then, the sample was cooled to 145 °C at a cooling rate of 30 °C min^{-1} and maintained there for 30 min. The isothermal crystallization morphology of different samples at 145 °C could be accordingly obtained. The Fourier transform infrared (FTIR) spectra of different samples were recorded at room temperature on a Nicolet 6700 Infrared spectrometer (Thermo Fisher Scientific) with a resolution of 4 cm^{-1}. The tensile and flexural tests were measured at ambient temperature using an Instron universal testing machine 4302 (Instron Corporation), according to ASTM D638 (crosshead speed 50 mm min^{-1}) and ASTM D790 (in a 3-point loading mode), respectively. The impact tests were done at ambient temperature on a 1400-z pendulum impact testing machine (New Sansi Material Company) according to ASTM D256 standard.

RESULTS AND DISCUSSION

Morphology Analysis

Figure 2(a,b) compares SEM images of PLA/HA/SMCW (2 wt %) and PLA/HA/SMCW (7 wt %) samples. As can be seen, for PLA/HA/SMCW sample (2.0 wt %), there are agglomerated HA nanoparticles poorly dispersed in PLA matrix. The interfacial combination of HA fillers with matrix is poor. Most HA nanoparticles break away from matrix upon sample fracturing due to the poor interface bonding. In addition, there are the obvious interface gaps found between whiskers and matrix, indicating that SMCWs also exhibit the weak adhesion to the matrix polymer. With increasing SMCW content to 7.0 wt %, relative to PLA/HA/SMCW (2.0 wt %) sample, the size of SMCW aggregates is much bigger and the interfacial compatibility becomes poorer (the more obvious interface gap).

In order to improve the dispersion of HA nanoparticles and the interfacial compatibility between fillers and matrix, addition of PLA-*g*-MAH as a compatibilizer was attempted so as to achieve the improvement in mechanical performance of PLA/HA/SMCW composite (SMCW content was fixed at 2.0 wt %). Figure 2(c) shows the SEM images of PLA-*g*-MAH compatibilized PLA/HA/SMCW system. As can be seen, compared with unmodified PLA/HA/SMCW sample [Figure 2(a)], the HA nanoparticles and whiskers at the fractured surface are wetted and closely encapsulated by PLA matrix. The interface becomes blurry. This shows that the interfacial combination is obviously improved. In addition, the dispersion of HA nanoparticle fillers becomes more homogeneously. Above results indicate that the incorporation of PLA-*g*-MAH effectively enhances the filler–

Table I. Compositions of PLA/HA and Various Whisker Reinforced PLA/HA Nanocomposites

Samples	PLA (wt %)	HA (wt %)	SMCW (wt %)	PLA-*g*-MAH (wt %)
PLA/HA	95.0	5.0	0.0	-
PLA/HA/SMCW (1.0 wt %)	94.1	4.9	1.0	-
PLA/HA/SMCW (2.0 wt %)	93.1	4.9	2.0	-
PLA/HA/SMCW (5.0 wt %)	90.2	4.8	5.0	-
PLA/HA/SMCW (7.0 wt %)	88.4	4.6	7.0	-
PLA/PLA-*g*-MAH/HA/SMCW (2.0 wt %)	85.6	4.9	2.0	7.5

Note: the weight ratio of PLA (or PLA+PLA-*g*-MAH) to HA keeps constant (95:5).

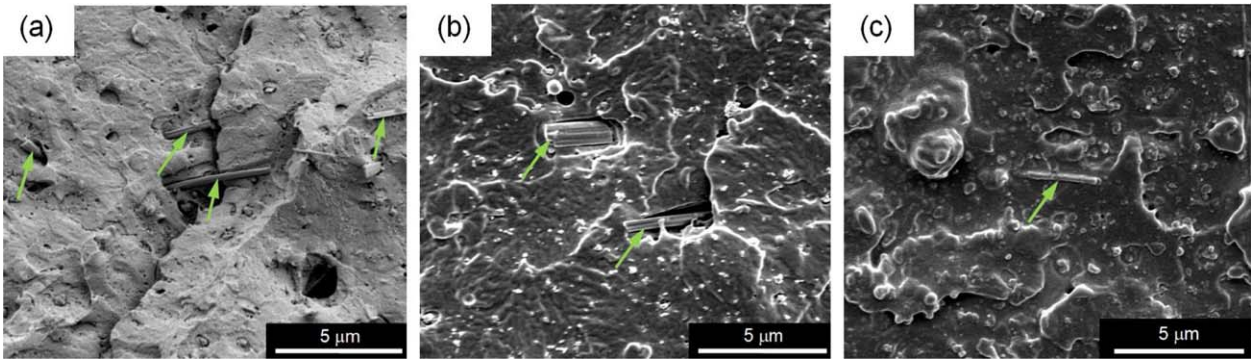

Figure 2. SEM photographs of PLA/HA/SMCW (2.0 wt %) (a), PLA/HA/SMCW (7.0 wt %) (b), and PLA/PLA-*g*-MAH/HA/SMCW (2.0 wt %) (c) nanocomposites. The arrows indicate the distributed SMCWs. [Color figure can be viewed in the online issue, which is available at wileyonlinelibrary.com.]

matrix interactions and remarkably improves the interfacial compatibility.

Dynamic Rheological Behavior

In dynamic rheology, the complex viscosity is an important parameter which can measure the viscoelasticity of material and reflect the energy dissipation in every oscillation cycle.[36,37] Figure 3 shows the complex viscosity curves of PLA/HA, PLA/HA/SMCW, and PLA/PLA-*g*-MAH/HA/SMCW nanocomposites at 180 °C. As can be seen, in the range of test frequency, the complex viscosities of all samples decrease with increase in angular frequency (ω). This shows that the melts of all the nanocomposites have the characteristics of pseudoplastic fluid. In addition, the incorporation of whiskers remarkably decreases the complex viscosity, e.g., the complex viscosities of whiskers contained systems are significantly lower than that of PLA/HA sample without whiskers, revealing that the added SMCWs could significantly improve the processability of system (it is experimentally found that the incorporation of SMCWs can really improve the extrusion and injection molding processability remarkably). This is a very interesting result and the reason for this deserves the further investigation. However, it is preliminarily believed that this is possibly because the incorporated rigid SMCWs increase the distance between the PLA macromolecular chains and hence reduce the entanglement interactions between polymer chains. This would make the macromolecular chain segments move more easily than those without SMCWs added at the same temperature. Consequently, the addition of whiskers would not deteriorate the processability but would improve it instead.

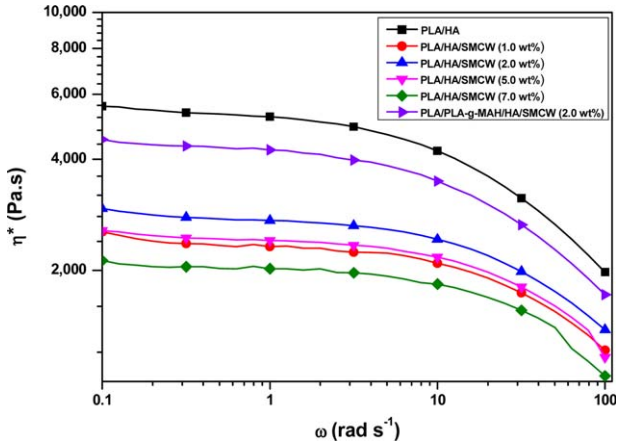

Figure 3. The relationship between complex viscosity and angular frequency for PLA/HA, PLA/HA/SMCW, and PLA/PLA-*g*-MAH/HA/SMCW nanocomposites. [Color figure can be viewed in the online issue, which is available at wileyonlinelibrary.com.]

The variation of dynamic rheological behavior of PLA/HA/SMCW nanocomposite with SMCW content shows a complicated trend, as is also shown in Figure 3. It is seen that the complex viscosity increases firstly and then decreases with increasing SMCW content. The maximum value occurs at 2.0 wt % SMCW loading. It is believed that although the presence of a small amount of SMCWs (<1.0 wt %) could decrease the viscosity of composite due to increase in distance between macromolecular chains, the viscosity is also related to the distribution of SMCWs. Generally, the higher the SMCW content is, the higher the aggregation degree would be. Based on SEM results (Figure 2), it is clear that the increase in SMCW content would lead to the heavier agglomeration of SMCW. When SMCW content increases to a value in the range of 1.0–2.0 wt %, the aggregates composed of SMCW and HA particles could possibly wrap a part of matrix resin. This would increase the local concentration of the dispersed phase filler particles (the effect of this factor causing increase in viscosity might be stronger than that causing decrease in viscosity due to the increased distance between polymer chains resulted from SMCW incorporation),[38] thus resulting in increase in viscosity of system. On the other hand, when SMCW content is higher than 2.0 wt %, the increase in the distance between macromolecular chains due to agglomeration of the rigid SMCW particles would be the predominating factor again. This, undoubtedly, would make the viscosity of composite decrease again. Very interestingly, relative to PLA/HA/SMCW sample, the complex viscosity of the PLA-*g*-MAH compatibilized system significantly increases. This is because the incorporation of PLA-*g*-MAH imparts the stronger bonding force to the interface between filler and matrix resin. Meanwhile, the maleic anhydride (MAH) groups of PLA-*g*-MAH macromolecular chains promote the entanglements between PLA matrix macromolecular chains. This would make polymer chains consume more energy under shear stress field, thus increasing the complex viscosity.

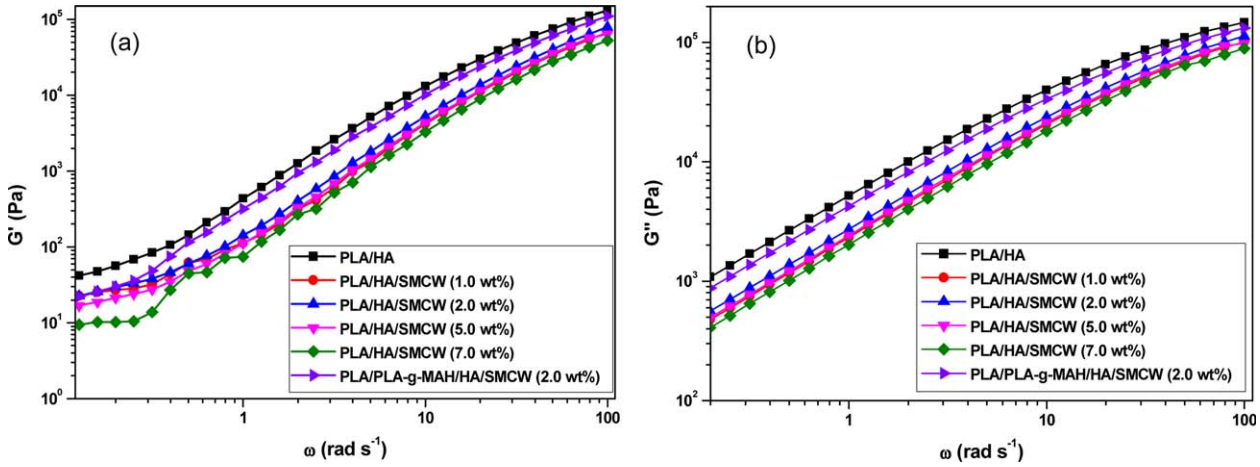

Figure 4. The viscoelastic parameters storage modulus G' (a) and loss modulus G'' (b) of PLA/HA, PLA/HA/SMCW and PLA/PLA-*g*-MAH/HA/SMCW nanocomposites as a function of angular frequency. [Color figure can be viewed in the online issue, which is available at wileyonlinelibrary.com.]

Figure 4 shows variation of the storage modulus (G') and loss modulus (G'') of various nanocomposites with angular frequency (ω). It is known that the storage modulus and loss modulus, characterizing the elastic property and viscous property of polymer material, respectively, are related to the energy storage and energy loss in deformation process of each cycle.[39] From Figure 4, it is seen that with decrease in ω, G' and G'' of all composites present decreasing tendency and G'' is higher than G'. This indicates that the prepared nanocomposites exhibit viscoelastic behavior where the viscous effect predominates. In addition, the dependence of G' of composite on ω deviates from the classical linear viscoelastic theory in the low frequency region and there is a special viscoelastic response with a feature of plateau occurring (particularly, with increase of SMCW content to 7 wt %, the well-defined plateau is much more obvious), i.e., the composites show some solid-like behaviors. This indicates that the movement of PLA macromolecular chains is strongly confined by the fillers and such a confinement is due to formation of network structures of filler particles in composite. Moreover, both G' and G'' of PLA/HA sample are higher than those of PLA/HA/SMCW and PLA/PLA-*g*-MAH/HA/SMCW samples, indicating that addition of whiskers effectively reduces the internal friction of polymer chains, decreases the adhesion effect of melt on mold and hence enhances the melt flowability. As a result, both G' and G'' of composites decrease. It is also noted that both G' and G'' of PLA-*g*-MAH compatibilized sample are significantly higher than those of uncompatibilized systems with different whisker content. However, for the latter, both G' and G'' of all the related samples are close. This indicates that in the PLA-*g*-MAH contained sample, the incorporation of PLA-*g*-MAH could increase the rigidity and internal friction of composite, i.e., effectively enhances the interactions between polymer chains and also the ones between polymer chains and fillers. This exactly reflects the compatibilizing effects of PLA-*g*-MAH.

Figure 5 shows the mechanical loss (loss angle tangent, tanδ)—dynamic frequency (ω) relationship curves of various samples. The mechanical loss (tanδ = G''/G') is related to the motion ability of polymer chains.[36] As can be seen, in the low frequency region (<1 rad s^{-1}), tanδ of PLA/HA/SMCW sample increases with increase in whisker content. This is possibly because the incorporation of whiskers promotes the movement of macromolecular chain segments and at the same frequency the amplitude of motion of polymer molecular chains augments, thus increasing mechanical loss. In the higher frequency region (>1 rad s^{-1}), the mechanical losses of PLA/HA/SMCW samples with different whisker content tend to be close and however is obviously higher than that of PLA/HA sample without whisker. This indicates that, when the angular frequency is higher than 1 rad s^{-1}, on one hand, the difference in mechanical loss between PLA/HA/SMCW samples with different whisker content would become small and on the other hand, the whisker incorporation would have remarkable influence on the dynamic rheological behavior when the whisker content is lower than a certain critical concentration. In addition, it is also noted that the mechanical loss of PLA/PLA-*g*-MAH/HA/SMCW sample is close to that of PLA/HA sample. This could be related to the fact that the incorporated PLA-*g*-MAH increases the viscous

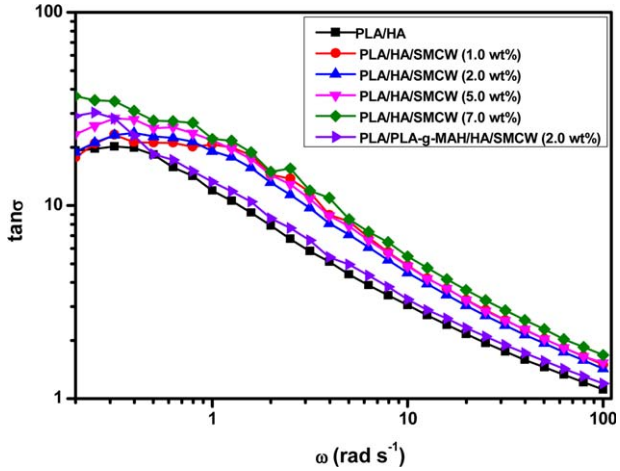

Figure 5. The variation of loss tangent tanδ of PLA/HA, PLA/HA/SMCW and PLA/PLA-*g*-MAH/HA/SMCW composites with the angular frequency ω. [Color figure can be viewed in the online issue, which is available at wileyonlinelibrary.com.]

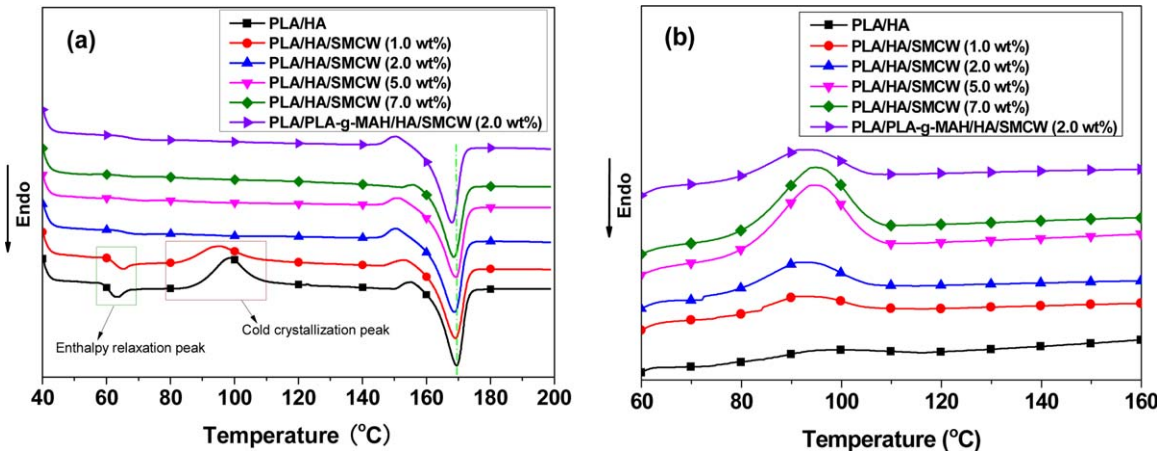

Figure 6. The DSC heating (a) and cooling (b) curves of PLA/HA, PLA/HA/SMCW, and PLA/PLA-*g*-MAH/HA/SMCW nanocomposites. [Color figure can be viewed in the online issue, which is available at wileyonlinelibrary.com.]

resistance of system and hence weakens the movement of polymer molecular chains.

Crystallization Behavior

Figure 6 shows the melting (a) and crystallization (b) curves of various samples. The corresponding DSC parameters are listed in Table II. It can be seen that there are four peaks occurring in DSC heating curve of PLA/HA sample, corresponding to enthalpy relaxation (62 °C, associated with the glass transition), cold crystallization (97 °C), crystal phase transition (155 °C), and crystallization melting peak (169 °C), respectively. In PLA/HA sample, the small endothermic peak occurring in glass transition region is caused by the enthalpy relaxation, which is associated with physical aging of PLA and can be attributed to the melting of the locally ordered domains formed during PLA aging process.[40,41] However, the incorporation of whiskers restrains the appearance of enthalpy relaxation. With increase of whisker content to 2.0 wt % or more, the enthalpy relaxation phenomenon even disappears. This indicates that the incorporated whiskers can effectively prevent the physical aging of PLA. The reason for this may be that the added rigid whiskers promote formation of the network structures of filler particles, which possibly prevent the formation of the locally ordered domains during aging process to a certain extent. At near 100 °C, there is an obvious cold crystallization exothermic peak occurring in PLA/HA sample. This is because the macromolecular chains of PLA matrix with slow crystallization rate have no time to be arranged into the lattice in molding process due to rapid cooling and hence cannot crystallize adequately. In the subsequent DSC heating process, the quenched macromolecular chains are unfrozen and arranged regularly and hence could be reorganized into the crystallization regions. The cold crystallization peak can reflect the crystallization capability of macromolecular chains to a certain degree. It is interesting that, with increase in whisker content, on one hand the cold crystallization temperature decreases and on the other hand the cold crystallization peak weakens and even disappears (whisker content $\geq$2.0 wt %), indicating that the added whiskers can hold back the cold crystallization of PLA and make the PLA crystallization more easy. The reason for this can be explained as follows. The rheological measurements mentioned before show that the incorporated rigid whiskers could reduce the entanglement of PLA polymer chains, which is beneficial to the regular arrangement of these PLA chains. This would make the PLA macromolecular chains, which could not crystallize before, is able to crystallize again upon cooling molding. As a result, in the subsequent DSC heating process the cold crystallization peak would weaken and even disappear. This indicates that the added whiskers can enhance the melt crystallization capability of PLA macromolecular chains, i.e., they are able to promote the regular arrangement of polymer chains and hence be beneficial to crystal growth.

Table II. Melting and Crystallization Parameters Obtained from DSC Curves of PLA/HA, PLA/HA/SMCW and PLA/PLA-*g*-MAH/HA/SMCW Nanocomposites

Samples	T_m (°C)	T_{co} (°C)	T_c (°C)	X_c (%)	ΔT (°C)
PLA/HA	169.8	116.4	95.0	2.5	74.5
PLA/HA/SMCW (1.0 wt %)	169.7	104.7	91.1	3.4	78.2
PLA/HA/SMCW (2.0 wt %)	169.7	104.9	91.2	6.6	78.0
PLA/HA/SMCW (5.0 wt %)	169.5	105.7	93.6	12.6	75.4
PLA/HA/SMCW (7.0 wt %)	169.2	105.8	94.3	12.8	74.6
PLA/PLA-*g*-MAH/HA/SMCW (2.0 wt %)	167.8	104.7	91.3	6.2	77.9

Note: T_{co}, T_c, X_c, and ΔT are onset crystallization temperature, crystallization temperature, crystallinity and supercooling degree, respectively; $X_c = \Delta H/\Delta H_0$. Where ΔH and ΔH_0 are melting enthalpy of sample and melting enthalpy of 100% crystallized pure PLA (93.7 J g^{-1}), respectively.

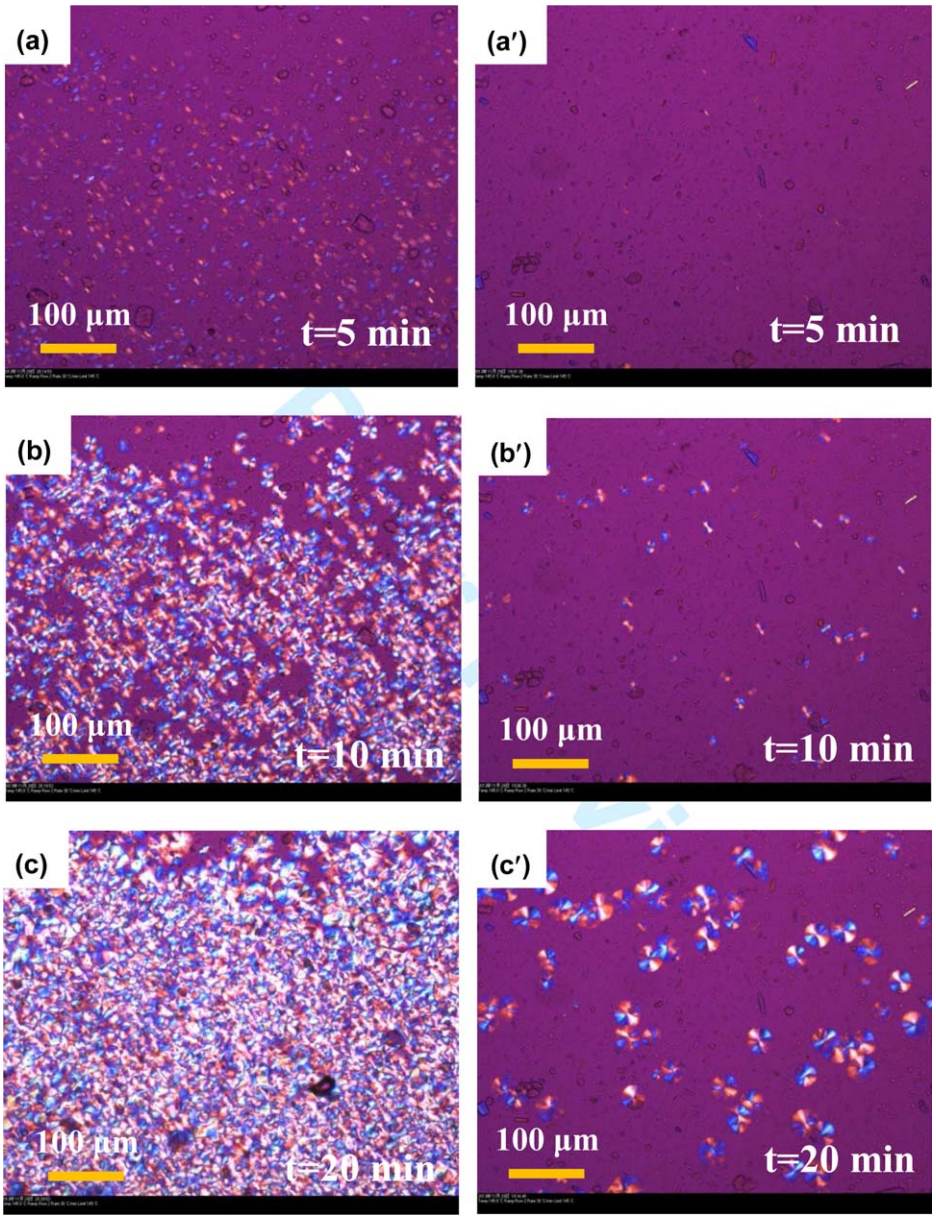

Figure 7. PLM images of PLA/HA (a–c) and PLA/HA/SMCW (2.0 wt %) (a′–c′) nanocomposites at 145 °C at different time: 5 min (a and a′), 10 min (b and b′), and 20 min (c and c′). [Color figure can be viewed in the online issue, which is available at wileyonlinelibrary.com.]

From Figure 6 and Table II, it is also seen that, the addition of whisker and increase of its content show small influence on the melt temperature of sample but big influence on onset crystallization temperature (T_{co}), crystallization temperature (T_c), and crystallinity (X_c). The incorporated whiskers with different loading (1.0–7.0 wt %) can all decrease T_{co} and T_c. But the T_c decrease degree for different loading of whiskers contained sample is also different. This suggests that the incorporation of different loading of whiskers has no heterogeneous nucleation effect on PLA but would inhibit the nucleation of PLA macromolecular chains to different degree (as is also confirmed by the later PLM observation). With increasing SMCW content, the corresponding T_c also increases (but still lower than that of PLA/HA). This indicates that the higher loading (5.0–7.0 wt %) of whiskers has the weaker inhibitive effect on the nucleation of polymer chains than the lower loading (1.0–2.0 wt %) of whiskers. This could be related to such a fact that the higher loading of whiskers have a relatively bigger aggregation degree, which can increase the distance between polymer chains and hence make the regular arrangement of macromolecular chains be more easy. Based on above analysis, it is clear that there are two opposite effects of whiskers on crystallization of PLA polymer chains, i.e., inhibition of nucleation and promotion of crystal growth, which could be related to the content and dispersion state of whiskers. With increasing the SMCW content, the X_c increases also. This is possibly because at the higher whisker loading the inhibition of nucleation becomes weakened and simultaneously the promotion of crystal growth is enhanced. It is also noted that, in the DSC cooling crystallization process, the addition of whiskers increases the supercooling

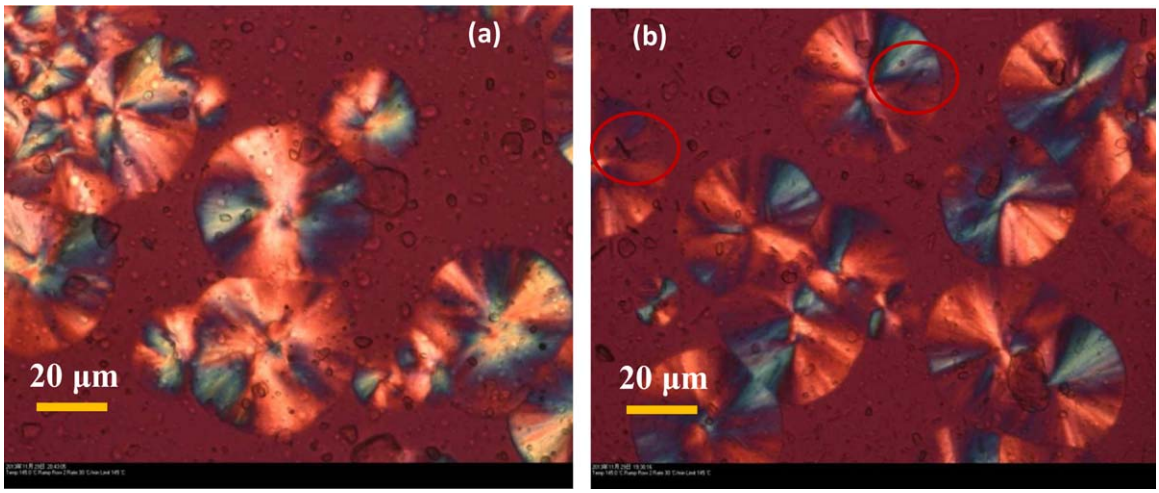

Figure 8. PLM images of PLA/HA (a) and PLA/HA/SMCW (b) nanocomposites after isothermally crystallized at 145 °C for 30 min. [Color figure can be viewed in the online issue, which is available at wileyonlinelibrary.com.]

degree (ΔT) (ΔT refers to the difference between equilibrium melting temperature and crystallization temperature). Previous studies revealed that the smaller ΔT is more advantageous to the crystallization of polymers.[42] This indicates that at the same cooling rate, PLA/HA sample could crystallize earlier than PLA/HA/SMCW sample and the former could generate crystal nucleus more easily. From Table II, it is also seen that, the introduced PLA-*g*-MAH decreases the melting temperature of samples, illustrating that the MAH groups of PLA-*g*-MAH could possibly restrict the movement of PLA macromolecular chains through their hydrogen bonding interactions with PLA and make PLA crystallize less perfectly. Compared with PLA/HA/SMCW sample, the addition of PLA-*g*-MAH has no significant effect on the crystallinity.

In order to further investigate the influence of whiskers incorporation on the crystallization of PLA in PLA/HA system, the polarized microscopy (PLM) analyses were carried out on PLA/HA and PLA/HA/SMCW (2 wt %) samples. Interestingly, at 150 °C and within 30 min, many growing PLA spherulites are observed in PLA/HA sample, but no crystal nucleus formation is observed in PLA/HA/SMCW sample. This illustrates that the incorporation of whiskers inhibits the nucleation of PLA macromolecular chains, which is in agreement with the DSC results. To better compare the crystal nucleation and crystal growth of PLA/HA with those of PLA/HA/SMCW, the crystallization temperature was decreased to 145 °C and PLM technique was also used to investigate the isothermal crystallization behavior at different time. The results are shown in Figure 7. As can be seen, in the same time interval, the density of the formed crystal nucleus of PLA/HA/SMCW is obviously lower than that of PLA/HA. With extension of the crystallization time, the formed spherulites gradually grow up. The spherulites of PLA/HA collide each other and deform due to their dense distribution. Comparatively, the spherulites of PLA/HA/SMCW are much more perfect. The final dimension of the spherulites in both samples is similar. Above analyses further illustrate that although the added whiskers affects the nucleation number, they do not prevent the movement of PLA macromolecular chains and the crystal growth.

Figure 8 shows the PLM photos of PLA/HA and PLA/HA/SMCW (2 wt %) samples isothermally crystallized at 145 °C for 30 min. As can be seen, both samples show the typical spherulite morphologies with the well-defined Maltese crosslike extinction pattern. In addition, comparing the PLM photos of both samples, it is seen that the incorporation of whiskers does not prevent the growth of crystals and the formed spherulites are more distinct [Figure 8(b)]. This further indicates that in the whiskers incorporated sample the growth of spherulite is more stable, the crystal defects are less and the formed spherulites are more perfect.

Mechanical Properties

Figure 9 shows the mechanical properties of PLA/HA sample and PLA/HA/SMCW samples with different whisker content. With increase in whisker content, the tensile strength increases firstly then decreases and the maximum value occurs at 2.0 wt % whisker loading (reaching 69.0 MPa, increased by 7.0% as compared with PLA/HA sample without whisker). It is further noted that, with increase in whisker content, the impact strength also increases firstly and then decreases and reaches the optimum value (16.4 kJ m^{-2}) at 2.0 wt % whisker loading [increased by 24% as compared with PLA/HA sample (13.3 kJ m^{-2})]. Besides, for flexural strength, with increase in whisker content, it exhibits a slowly increasing tendency (reaching 99.0 MPa at 7.0 wt % whisker loading, increased by 11.0% as compared with PLA/HA sample). Above results show that a small amount of the incorporated inorganic whiskers could exhibit both reinforcing and toughening effects. When the whisker content is at 2.0 wt %, the prepared PLA/HA/SMCW nanocomposite could have the best comprehensive performance.

The improvement in mechanical performance of whiskers reinforced PLA/HA nanocomposite is limited due to the uncompatibilized interface. So, it is necessary to use modifier to enhance the interfacial adhesion. PLA-*g*-MAH was accordingly used. The results are shown in Figure 10. As can be seen, compared with the unmodified PLA/HA/SMCW sample, there are substantial increases in all the mechanical properties (including tensile

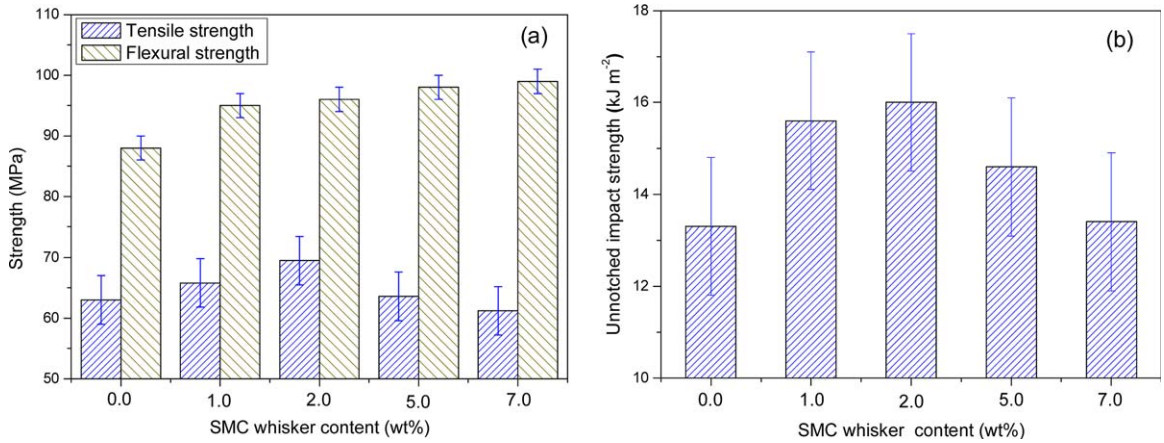

Figure 9. Effect of whisker content on the mechanical properties of PLA/HA/SMCW nanocomposites: tensile and flexural strength (a) and unnotched impact strength (b). [Color figure can be viewed in the online issue, which is available at wileyonlinelibrary.com.]

strength, flexural strength, and impact strength) of PLA/PLA-*g*-MAH/HA/SMCW sample (the tensile strength, flexural strength and unnotched impact strength have been further increased from 69.0, 96.2, and 16.0 to 91.2 MPa, 124.6 MPa and 25.7 kJ m^{-2}, respectively. The increase degree reaches 32.2, 29.5, and 60.6%, respectively). Above encouraging results show that incorporation of PLA-*g*-MAH could remarkably improve the mechanical properties (particularly the impact property) of PLA/HA/SMCW nanocomposite, which shows the good application prospect. For PLA-*g*-MAH compatibilized system, there are the maleic anhydride (MAH) groups on the macromolecular chains of PLA-*g*-MAH, which can participate in the interfacial reaction. On one hand, the grafted MAH groups can possibly have interfacial esterification reactions with the hydroxyls on the surface of fillers HA and whiskers; on the other hand, the bone macromolecular chains of PLA-*g*-MAH can be closely entangled and hence well compatibilized with the same bone macromolecular chains of PLA matrix resin. As a result, the interfacial bonding could be significantly enhanced. The interfacial compatibilizing mechanism of PLA-*g*-MAH above mentioned could be well illustrated using Figure 11. Since the good PLA–filler interfacial adhesion can overcome formation of the micro cracks between PLA matrix and whiskers, the mechanical performance (particularly the impact strength being representative of the toughness to a certain degree, a very important physical property) of PLA/HA composite could be effectively augmented.

In order to confirm the interfacial compatibilizing mechanism of PLA-*g*-MAH above proposed (the interfacial esterification reactions between PLA-*g*-MAH and SMCW/HA fillers), the FT-IR measurements were carried out. The results are shown in Figure 12. The attribution of the featured absorptions of PLA and PLA-*g*-MAH has been involved in the experimental part. For HA, the peak at 3564 cm^{-1} can be attributed to the stretching vibration absorption of O—H group in OH^-. The absorptions at 3401 and 1632 cm^{-1} are caused by the stretching vibration and the bending vibration of —OH groups in H_2O adsorbed on HA, respectively. The bands in the range of 960–1090 cm^{-1} are ascribed to the featured absorptions of PO_4^{3-} group. Due to the low content of HA, the featured absorption of HA are covered by the strong absorptions of PLA in PLA/HA and PLA/HA/SMCW samples. However, for the FT-IR spectrum of PLA-*g*-MAH contained PLA/HA/SMCW sample, there are new peaks occurring at 1309 cm^{-1} and in the range of 1590–1660 cm^{-1}, which could be attributed to the stretching vibration absorption of Si—O—C group and the vibration absorption

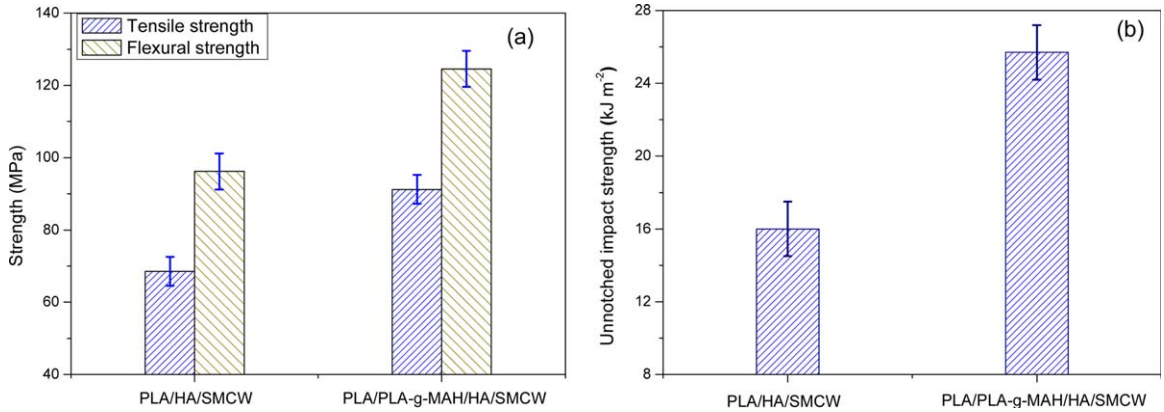

Figure 10. The mechanical properties of PLA/HA/SMCW and PLA/PLA-*g*-MAH/HA/SMCW nanocomposites: tensile and flexural strength (a) and unnotched impact strength (b). [Color figure can be viewed in the online issue, which is available at wileyonlinelibrary.com.]

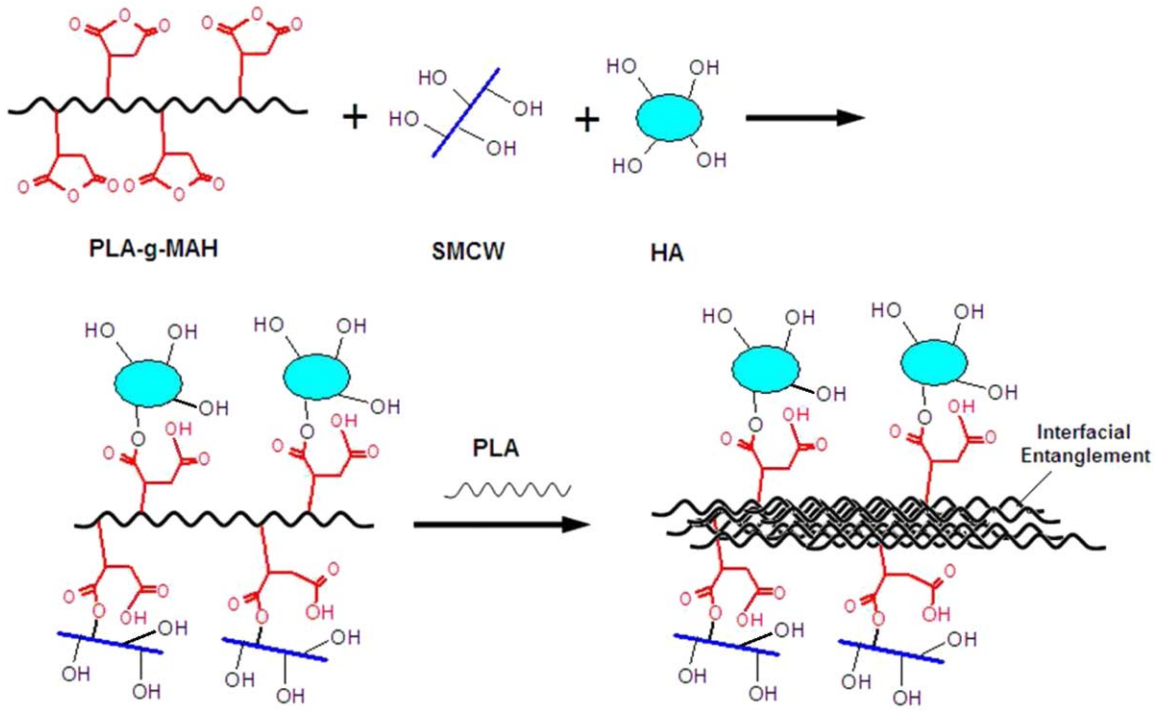

Figure 11. The proposed mechanism of compatibilizing effect of PLA-*g*-MAH in PLA/PLA-*g*-MAH/HA/SMCW nanocomposite system. [Color figure can be viewed in the online issue, which is available at wileyonlinelibrary.com.]

of C—O group in ester group, respectively. This shows the existence of the possible interfacial esterification reactions between PLA-*g*-MAH and SMCW/HA fillers.

CONCLUSIONS

In this paper, the SiO_2—MgO—CaO inorganic whiskers were used to reinforce PLA/HA nanocomposites. Meanwhile, PLA-*g*-MAH was adopted to enhance the interfacial compatibility. In the uncompatibilized PLA/HA/SMCW nanocomposite, the dispersion of HA nanoparticles and the filler–PLA matrix interfacial adhesion are both poor. The introduction of PLA-*g*-MAH proves to remarkably enhance the interfacial compatibility and the filler dispersion. The dynamic rheological experiments verify that the incorporation of an appropriate amount of whiskers obviously decreases the complex viscosity. This would be beneficial to improvement in the processability of system. However, the addition of PLA-*g*-MAH obviously increases the complex viscosity. The crystallization results show that the introduced whiskers have the inhibitive effect on the nucleation of PLA macromolecular chains. The inhibition degree is depended on the content of whiskers. On the other hand, the incorporated whiskers also effectively prevent the occurrence of PLA cold crystallization, showing the introduced whiskers can enhance the melt crystallization capability of PLA. The PLM observations further confirm the inhibitive effect of whiskers on the nucleation of PLA polymer chains. However, they do not restrain the growth of crystals. Only addition of an appropriate amount of whiskers can reinforce and toughen the PLA/HA nanocomposite. The incorporation of PLA-*g*-MAH can further enhance the mechanical properties of the reinforced nanocomposites to a considerable degree.

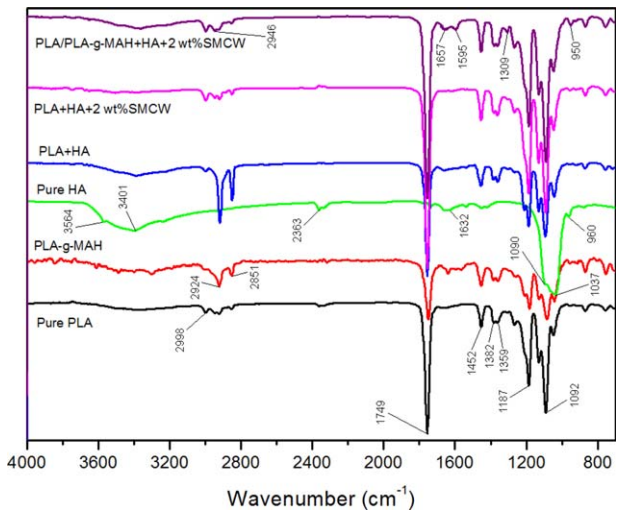

Figure 12. The FT-IR spectra of pure PP, PLA-*g*-MAH, pure HA, PLA/HA, PLA/HA/SMCW, and PLA/PLA-*g*-MAH/HA/SMCW samples. [Color figure can be viewed in the online issue, which is available at wileyonlinelibrary.com.]

ACKNOWLEDGMENTS

This work was kindly supported by the National Natural Science Foundation of China (51421061 and 51433006), the International Science and Technology Cooperation Program of China (2013DFG52300) and the Program of Introducing Talents of Discipline to Universities (B13040).

REFERENCES

1. Hughes, J.; Thomas, R.; Byun, Y.; Whiteside, S. *Carbohydr. Polym.* **2012**, *88*, 165.
2. Mohammad, S.; Long, J.; Mohammad, A.; Ismail, G. *J. Appl. Polym. Sci.* **2012**, *129*, 1735.
3. Fan, Y. Q.; Zhu, J. Y.; Chen, S. F.; Chen, X. S.; Yin, J. B. *Polymer* **2015**, *67*, 63.
4. Lizundia, E.; Vilas, J. L.; Leon, L. M. *Carbohydr. Polym.* **2015**, *123*, 256.
5. Nagarajan, V.; Zhang, K. Y.; Misra, M.; Mohanty, A. K. *ACS Appl. Mater. Interfaces* **2015**, *7*, 11203.
6. Lin, L.; Deng, C.; Lin, G. P.; Wang, Y. Z. *Indus. Eng. Chem. Res.* **2015**, *54*, 5643.
7. Furuhashi, Y.; Kimura, Y.; Yamane, H. *J. Polym. Sci. B: Polym. Phys.* **2007**, *45*, 218.
8. Rajan, S. S.; Turovskiy, Y.; Singh, Y.; Chikindas, M. L.; Sinko, P. J. *J. Control. Release* **2014**, *194*, 301.
9. Kanno, T.; Oyama, H. T.; Usugi, S. *Eur. Polym. J.* **2014**, *54*, 62.
10. Uehara, H.; Karaki, Y.; Wada, S.; Yamanobe, T. *ACS Appl. Mater. Interfaces* **2010**, *2*, 2707.
11. Xu, Z. H.; Niu, Y. H.; Yang, L.; Xie, W. Y.; Li, H.; Gan, Z. H.; Wang, Z. G. *Polymer* **2010**, *51*, 730.
12. Shi, Q. F.; Zhou, C. J.; Yue, Y. Y.; Guo, W. H.; Wu, Y. Q.; Wu, Q. L. *Carbohydr. Polym.* **2012**, *90*, 301.
13. Lu, L.; Peter, S. J.; Lyman, M. D.; Lai, H. L.; Leite, S. M.; Tamada, J. A.; Vacanti, J. P.; Langer, R.; Mikos, A. G. *Biomaterials* **2000**, *21*, 1595.
14. Cumkur, E. A.; Baouz, T.; Yilmazer, U. *J. Appl. Polym. Sci.* **2015**, *132*, 42553.
15. Barletta, M.; Puopolo, M.; Tagliaferri, V.; Vesco, S. *J. Appl. Polym. Sci.* **2016**, *133*, 42252.
16. Wang, H.; Sun, X. Z.; Seib, P. *J. Appl. Polym. Sci.* **2001**, *82*, 1761.
17. Hasegawa, S.; Neo, M.; Tamura, J.; Fujibayashi, S.; Takemoto, M.; Shikinami, Y.; Okazaki, K.; Nakamura, T. *J. Biomed. Mater. Res. A* **2007**, *81*, 930.
18. Park, S. H.; Park, S. H.; Park, D. S.; Kang, Y. G.; Shin, J. W.; Kim, H. K.; Yoon, T. R.; Shin, J. W. *Tissue Eng. Regen. Med.* **2013**, *10*, 71.
19. Loo, S. C.; Moore, T.; Banik, B.; Alexis, F. *Curr. Pharm. Biotechnol.* **2010**, *11*, 333.
20. Jiang, L. Y.; Xiong, C. D.; Jiang, L. X.; Xu, L. J. *Thermochim. Acta* **2013**, *565*, 52.
21. Shen, L.; Yang, H.; Ying, J.; Ying, J.; Qiao, F.; Peng, M. *J. Mater. Sci. Mater. Med.* **2009**, *20*, 2259.
22. Zhou, H.; Touny, A. H.; Bhaduri, S. B. J. *Master. Sci. Mater. Med.* **2011**, *22*, 1183.
23. Chuenjitkuntaworn, B.; Supaphol, P.; Pavasant, P.; Damrongsri, D. *Polym. Int.* **2010**, *59*, 227.
24. Zong, C.; Qian, X. D.; Tang, Z.; Hu, Q. H.; Chen, J. R.; Gao, C. Y.; Tang, R. K.; Tong, X. M.; Wang, J. F. *J. Biomed. Nanotechnol.* **2014**, *10*, 1091.
25. Dadbin, S.; Naimian, F. *Polym. Int.* **2014**, *63*, 1063.
26. Zheng, F. Y.; Wang, S.; Wen, S. H.; Shen, M. W.; Zhu, M. F.; Shi, X. Y. *Biomaterials* **2013**, *34*, 1402.
27. Persson, M.; Lorite, G. S.; Cho, S. W.; Tuukkanen, J.; Skrifvars, M. *ACS Appl. Mater. Interfaces* **2013**, *5*, 6864.
28. Liu, C.; Chan, K. W.; Shen, J.; Wong, H. M.; Yeung, K. W. K.; Tjong, S. C. *RSC Adv.* **2015**, *5*, 72288.
29. Dinh, T. M. T.; Trang, P. T. T.; Huong, H. T.; Nam, P. T.; Phuong, N. T.; Trang, N. T. T.; Hoang, T.; Lam, T. D. *Int. J. Nanotechnol.* **2015**, *12*, 391.
30. Hu, Y.; Gu, X. Y.; Yang, Y.; Huang, J.; Hu, M.; Chen, W. K.; Tong, Z.; Wang, C. Y. *ACS Appl. Mater. Interfaces* **2014**, *66*, 17166.
31. Ning, N. Y.; Luo, F.; Pan, B. F.; Zhang, Q.; Wang, K.; Fu, Q. *Macromolecules* **2007**, *40*, 8533.
32. Su, R.; Wang, K.; Ning, N. Y.; Chen, F.; Zhang, Q.; Wang, C. Y.; Fu, Q.; Na, B. *Compos. Sci. Technol.* **2010**, *70*, 685.
33. Gao, Y.; Ren, K.; Ning, N. Y.; Fu, Q.; Wang, K.; Zhang, Q. *Polymer* **2012**, *53*, 2792.
34. Ishihara, Y.; Kyono, H.; Kohyama, N.; Otaki, N.; Serita, F.; Toya, T.; Kagawa, J. *Inhal. Toxicol.* **1999**, *11*, 131.
35. Rodelsperger, K.; Bruckel, B. *Inhal. Toxicol.* **2006**, *18*, 623.
36. Yan, Y. H.; Zhang, J. F.; Cui, J.; Cheng, J. M.; Liu, J. W. *Colloid. Polym. Sci.* **2012**, *290*, 1293.
37. Wu, D. F.; Zhou, C. X.; Hong, Z.; Mao, D. L.; Bian, Z. *Eur. Polym. J.* **2005**, *41*, 2199.
38. Lu, H. B.; Yang, Y. L. *Polym. Bull.* **2001**, *6*, 18.
39. Lee, K. H.; Lim, S. J.; Kim, W. N. *Macromol. Res.* **2014**, *22*, 624.
40. Frone, A. N.; Berlioz, S.; Chailan, J. F.; Panaitescu, D. M. *Carbohydr. Polym.* **2013**, *91*, 377.
41. Wei, J. C.; Sun, J. R.; Wang, H. J.; Chen, X. S.; Jing, X. B. *Chinese J. Polym. Sci.* **2010**, *28*, 499.
42. Jia, L. S.; Peng, L.; Chen, Y.; Mo, S. P.; Li, X. *Appl. Energ.* **2014**, *124*, 248.